Evolution of Hominin Detoxification: Neanderthal and Modern Human Ah Receptor Respond Similarly to TCDD

Jac M.M.J.G. Aarts,* ,[1,2] Gerrit M. Alink,[1] Henk J. Franssen,[2] and Wil Roebroeks[1]

[1]Human Origins Group, Faculty of Archaeology, Leiden University, Leiden, The Netherlands
[2]Laboratory of Molecular Biology, Department of Plant Sciences, Wageningen University, Wageningen, The Netherlands

*Corresponding author: E-mail: jac.aarts@wur.nl.
Associate editor: Connie Mulligan

Abstract

In studies of hominin adaptations to fire use, the role of the aryl hydrocarbon receptor (AHR) in the evolution of detoxification has been highlighted, including statements that the modern human AHR confers a significantly better capacity to deal with toxic smoke components than the Neanderthal AHR. To evaluate this, we compared the AHR-controlled induction of cytochrome P4501A1 (*CYP1A1*) mRNA in HeLa human cervix epithelial adenocarcinoma cells transfected with an Altai-Neanderthal or a modern human reference AHR expression construct, and exposed to 2,3,7,8-tetrachlorodibenzo-*p*-dioxin (TCDD). We compared the complete *AHR* mRNA sequences including the untranslated regions (UTRs), maintaining the original codon usage. We observe no significant difference in *CYP1A1* induction by TCDD between Neanderthal and modern human AHR, whereas a 150–1,000 times difference was previously reported in a study of the *AHR* coding region optimized for mammalian codon usage and expressed in rat cells. Our study exemplifies that expression in a homologous cellular background is of major importance to determine (ancient) protein activity. The Neanderthal and modern human dose–response curves almost coincide, except for a slightly higher extrapolated maximum for the Neanderthal AHR, possibly caused by a 5′-UTR G-variant known from modern humans (rs7796976). Our results are strongly at odds with a major role of the modern human AHR in the evolution of hominin detoxification of smoke components and consistent with our previous study based on 18 relevant genes in addition to *AHR*, which concluded that efficient detoxification alleles are more dominant in ancient hominins, chimpanzees, and gorillas than in modern humans.

Key words: Ah receptor (AHR), evolution of detoxification, Neanderthals, hominins, fire usage, smoke toxicity.

Introduction

The use of fire is a defining characteristic of the human lineage, with pyrotechnology being one of the most powerful tools developed during human evolution. Fire afforded humans with benefits affecting many domains of the human niche, including diet, defense against predators, thermoregulation, and social interaction (Carmody and Wrangham 2009; Wrangham 2009; Wiessner 2014).

However, pyrotechnology also came with (lesser known) costs (Henry et al. 2018), including toxicological ones (Aarts et al. 2016). The utilization of fire fueled with wood or other types of biomass on a daily basis implies frequent exposure to toxic components of smoke, to which polycyclic aromatic hydrocarbons (PAHs) contribute importantly (Freeman and Cattell 1990). In view of the well-known reproduction-toxic effects of tobacco smoke (DeMarini 2004; Dechanet et al. 2011) and the very similar composition of smoke from burning any type of biomass (Mishra et al. 2005; Naeher et al. 2007), the capacity to detoxify smoke toxicants is a crucial fitness factor inferred to have been under positive genetic selection in hominin populations ever since they started using open fire regularly.

The chronology of fire use is unclear: Some scholars advocate a long chronology, with routine fire use starting with *Homo erectus*, more than 2 Ma (Wrangham 2009; Wrangham and Carmody 2010). Based on archaeological data, others see consistent fire use as a significantly later phenomenon, from around 350,000 years ago onward (Roebroeks and Villa 2011; Shimelmitz et al. 2014), whereas regular fire production has even been inferred to be a modern human accomplishment only (Sandgathe et al. 2011); but see Sorensen (2017) and Sorensen et al. (2018). In an attempt to shed independent light on the debated chronology, Aarts et al. (2016) hypothesized that frequent exposure to toxic compounds occurring in smoke would have resulted in genetic adaptations in genes involved in detoxification of these toxicants. They analyzed 36 genetic variants in a comprehensive set of 19 relevant genes in Neanderthal, Denisovan, and (pre)historic and extant anatomically modern human genomes. This study showed that archaic hominins predominantly possessed protective gene variants, as do extant chimpanzees and gorillas. In contrast, the number of less protective, "high-risk" alleles has increased in modern humans. This pattern starts with the earliest modern human genome, of the Ust'-Ishim individual from 45,000 years ago

(Fu et al. 2014), and is suggestive of a deterioration in the ability to deal with smoke toxicants in modern humans, starting long before the emergence of agriculture. The more efficient detoxification of smoke toxins by Neanderthals and Denisovans was apparently hitchhiking on old primate mechanisms likely involved in dealing with plant toxins, and possibly in balancing certain photooxidation products induced by exposure to UV light (Wincent et al. 2012).

Cytochrome P450 1A1 (CYP1A1) plays an important, dualistic role in the defense against PAH intoxication, being involved both in phase 1 detoxification of PAHs and, along with this reaction, in the generation of mutagenic radical-type intermediates (Nebert et al. 2013; Divi et al. 2014). The CYP1A1 gene is under transcriptional control of the aryl hydrocarbon or Ah receptor (AHR) (Corchero et al. 2001; Nukaya and Bradfield 2009), a ligand-activated key regulator of many detoxification genes (Köhle and Bock 2007). In addition to dioxins and dioxin-like compounds such as 2,3,7,8-tetrachlorodibenzo-p-dioxin (TCDD), and PAHs such as benzo[a]pyrene (BaP), the AHR is activated by a very diverse range of agonist molecules (Denison et al. 2011). Therefore, the AHR gene variant and the resulting detoxification phenotype of ancient hominins are an important aspect of the evolution of smoke detoxification.

Starting from an evolutionary hypothesis comparable to Aarts et al. (2016), Hubbard et al. (2016) focused on the AHR gene, for which humans display a fixed difference (Val381) from the Neanderthal and Denisovan (Ala381) ancestral variant. Hubbard et al. (2016) performed an analysis of the modern human versus the Neanderthal AHR in rat cells and concluded that the Neanderthal AHR induced CYP1A1 mRNA expression with an effective concentration 50% (EC_{50}) between 150- and 1,000-fold lower than observed with the human AHR, implying a profound evolutionary change.

Here we report a complementary study following their approach and focusing on the AHR, but with important differences in experimental setup based on the literature on AHR biology and function (Okey et al. 1989; Ema, Ohe, et al. 1994; Poland et al. 1994; Pohjanvirta et al. 1998; Moriguchi et al. 2003), in particular the reported impaired signaling by the human AHR in a nonhuman cellular background attributed to cofactor incompatibility issues (Moriguchi et al. 2003). Furthermore, it is well documented that the 5'- and 3'-untranslated regions (UTRs) of a gene transcript may be involved in expression regulation of its gene product, mainly by affecting the translation rate and/or the stability of the transcript (Hinnebusch et al. 2016; Mayr 2017). Consequently, variations in the UTR sequence were found to be involved in the etiology of human diseases, including relatively rare neurologic disorders such as X-linked Charcot–Marie–Tooth disease, but also more common morbidities such as Alzheimer's dementia, and breast and other types of cancer (Chatterjee and Pal 2009), corroborating their potential importance.

These previously reported observations and mechanistic considerations prompted us to apply a modified setup. Most importantly, we chose to test the complete Neanderthal AHR mRNA sequence in a human instead of a rat cellular background. Therefore we included the 3'- and 5'-UTR in the AHR sequences compared, comprising four instead of two single-nucleotide variants (SNVs) while leaving the original codon usage intact. These modifications led to a very different result: No physiologically relevant difference in CYP1A1 transcription activation was observed between the ancient and modern AHR variants, which disagrees with a major role for the AHR in the evolution of smoke detoxification. This finding is consistent with our previous risk profiling study of hominin detoxification gene variants (Aarts et al. 2016).

Results

The Ancient and Modern AHR mRNA Sequences Studied Differ at Four Positions

To determine the degree of sequence identity between the ancient hominin and modern human AHR mRNAs, we compared the ancient AHR genomic sequences with the human reference genome (assembly GRCh38/hg38). The splicing donor and acceptor sites and ten adjacent bases upstream and downstream of the 20 exon–intron borders in the modern AHR reference transcript (Ensembl ID: ENST00000242057.8) were represented with 100% fidelity in the Altai- and Vindija-Neanderthal and Denisovan AHR gene, and were even very conserved from deeper down the primate lineage, justifying to assume no differences in the exon structure of the ancient and modern AHR transcripts studied here. Comparison of the ancient AHR mRNA sequences thus deduced from the published genomic sequences (supplementary material S10, Supplementary Material online) with the human reference genome revealed differences at six positions (fig. 1). The SNVs observed in the three ancient hominin sequences (Altai- and Vindija-Neanderthal and Denisovan) were almost identical except for position 73 in the 5'-UTR, where the Vindija-Neanderthal was heterozygous, but the C-allele was still matching the ancient hominin consensus and therefore chosen to be tested; and furthermore, at position 5439 of the 3'-UTR the Neanderthals seem to have acquired a lineage-specific A deletion variant, since it is found in both the Altai- and Vindija-Neanderthal genomes (in the heterozygous state), whereas it seems absent in the Denisovan. Hence, the 5438–5439 CA allele was found most representative for the available ancient genomes and therefore studied here. Altogether, as the ancient variants at positions 73 and 5438–5439 chosen were identical to the modern human reference, four sites remained different between the ancient and modern AHR mRNA sequences studied. Supplementary material S1, Supplementary Material online, shows an alignment of all sequences studied here and by Hubbard et al. (2016).

The HeLa Cell Strain Used Is Suitable for AHR Variant Testing

The human cervix epithelial adenocarcinoma cell line HeLa has been reported as a cell system with very low endogenous AHR expression validated for testing AHR gene variants (Koyano et al. 2005). Other studies, including this one (supplementary material S4, Supplementary Material online),
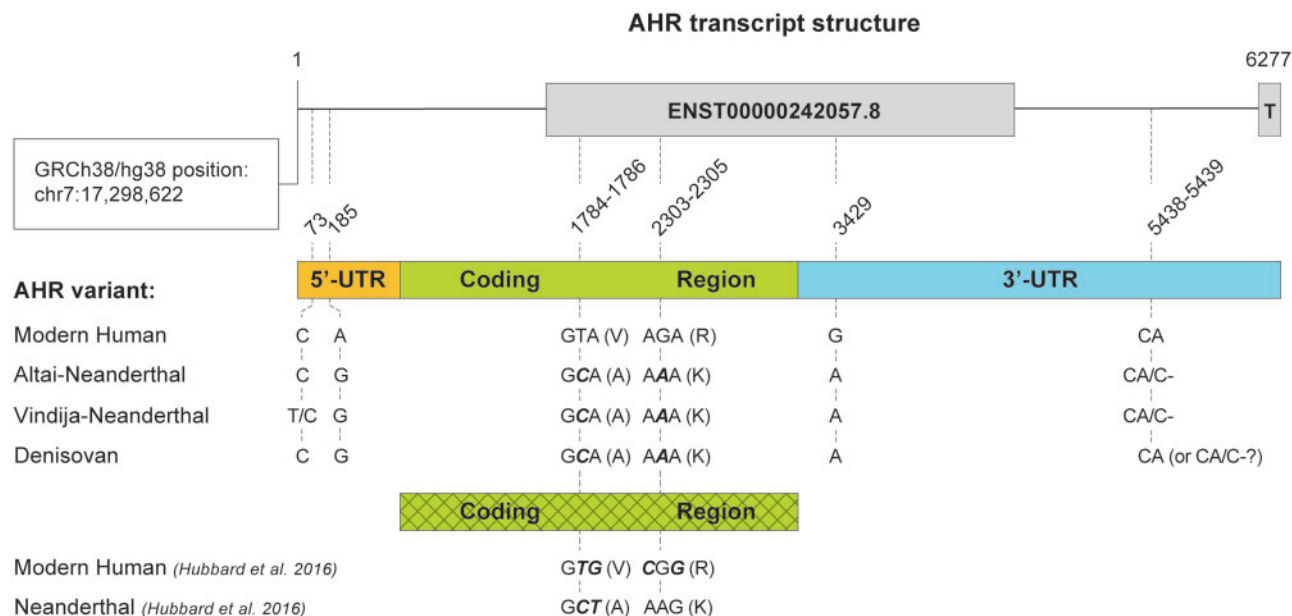
FIG. 1. Map of the modern human and ancient hominin *AHR* mRNA sequence variants studied here and by Hubbard et al. (2016). The modern human *AHR* variant tested was based on manually expert-curated sequence information from the Ensembl and RefSeq databases (details in Materials and Methods). The bar gives a scaled representation of this 6,277-bp sequence including the 5'-UTR, the AHR protein-coding region, and the 3'-UTR. The numbers above are the coordinates of the variant sites within the Ensembl *AHR* reference transcript ENST00000242057.8. Below it, the base, or codon plus encoded amino acid (V, valine; A, alanine; R, arginine; K, lysine) present in each *AHR* variant is indicated. Cross-hatching indicates optimization for mammalian codon use and minimal secondary mRNA structure; absence of hatching indicates that the codon usage from the human reference sequence is maintained. Codon bases in bold italics differ naturally, respectively, in the synthetic sequences tested by Hubbard et al. (2016), have been changed as compared with the modern human reference. Apart from the indicated variable sites the reported ancient *AHR* transcript sequences are identical to the modern reference sequence (see supplementary materials S1 and S10, Supplementary Material online).

generally report lower (Vorrink et al. 2014) to much lower (Singh et al. 1996) *AHR* mRNA or protein expression than in liver-derived cell lines. To further corroborate the suitability of the HeLa cell strain used in this study we transfected these cells with the empty pcDNA3.1/Zeo(+) vector used to construct expression vectors for the AHR variants to be compared, and measured the level of *AHR* mRNA overexpression achieved in this cell strain upon transfection with the constructed Neanderthal and modern human AHR expression vectors (details in Materials and Methods). We hold the view that the level of exogenous AHR overexpression is, in fact, the key factor in this experimental setup, not the background response as such. We observed a more than 1 order of magnitude (17–141 times) increase in the *AHR* mRNA level upon transfection with the AHR expression constructs as compared with empty vector (see supplementary material S4, Supplementary Material online). The excess of exogenous AHR will obviously outcompete the endogenously expressed receptor and largely prevent it from taking part in signal transduction. Expression of the Ah receptor repressor (AHRR) was reported to be relatively high in HeLa cells (Tsuchiya et al. 2003) and reduce CYP1A1 inducibility, but AHRR will be similarly outcompeted, because it is binding to the same dioxin-responsive element (DRE) as the AHR, resulting in an inducibility of 2–4 times (supplementary material S4, Supplementary Material online) as reported before (Nakajima et al. 2003). Moreover, we applied mathematical modeling of the contribution by the exogenous and endogenous AHR to

the overall *CYP1A1* induction response to demonstrate that this level of overexpression is amply sufficient to reveal a range of EC_{50} differences from as low as 10 times up to 1,000 times (supplementary material S4, Supplementary Material online). Our goal was to compare the transactivation capacity of the modern human and Neanderthal AHR variants including any possible effect of these variants on *AHR* mRNA or protein expression. One of the SNVs studied here (A/G at position 185 of the 5'-UTR) is known as an extant polymorphism (rs7796976) reported to affect *AHR* mRNA levels (Prager et al. 2016). The relevant experimental factor to carefully control is therefore the copy number of AHR expression constructs introduced into cells. We have applied two independent controls to ensure that this would not differ significantly between the HeLa cells transfected with the modern human and the Neanderthal AHR expression constructs: 1) cotransfection with an enhanced green fluorescent protein (EGFP) expression vector, enabling to visualize the transfection efficiency by fluorescence microscopy (fig. 2a–f); and 2) quantitative polymerase chain reaction (qPCR) of the mRNA expressed from the zeocin resistance gene expression cassette (ZEO) present on the backbone of the AHR expression constructs, which is a quantifiable measure proportional to the copy number of functional AHR expression constructs inside cells (fig. 2g). This approach avoids measuring expression vector molecules that were carried over during cell harvesting, or were damaged.
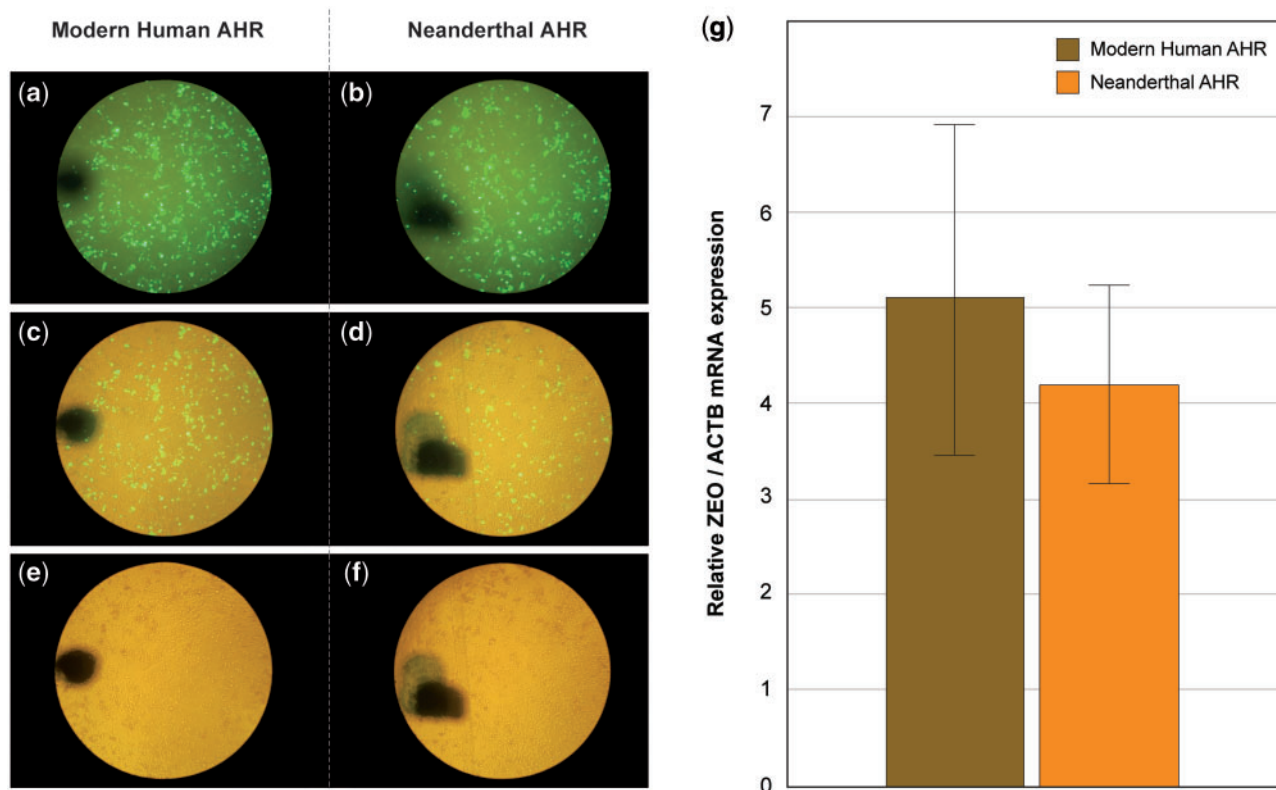
FIG. 2. HeLa cells were transfected with a pcDNA3.1/Zeo(+)-based expression construct for the complete modern human (panels *a, c, e*) or Neanderthal *AHR* mRNA (panels *b, d, f*). Panel *a–f*) Cotransfection (1:1 w/w) with the EGFP expression plasmid pcDNA3-EGFP to visualize the transfection efficiency; *a, b*) EGFP fluorescence; *c, d*) EGFP fluorescence + phase-contrast transillumination; *e, f*) transillumination only; the black marker spot is applied for orientation. The pcDNA3.1/Zeo(+) vector backbone is carrying a zeocin resistance gene expression cassette (ZEO). Therefore, ZEO mRNA expression is proportional to the number of functional construct molecules inside the cells upon transfection and allows to quantify the transfection efficiency by qRT-PCR. To correct for possible differences in cDNA input, the ZEO mRNA levels as quantified by qRT-PCR were normalized for β-actin (*ACTB*) mRNA expression and the mean and standard error of the mean (SEM) of the ZEO/*ACTB* mRNA ratio ($n = 13$) was plotted (panel *g*). A *t*-test on the difference in mean ratio between the transfections with the modern human and Neanderthal *AHR* expression constructs showed no significant difference ($P < 0.648$).

We took note of preliminary observations that HeLa cells also showed *CYP1A1* induction upon transfection with the AHR expression constructs without cotransfection with an Ah receptor nuclear translocator (ARNT) expression construct. We therefore measured the endogenous *ARNT* mRNA level in HeLa and in HepG2 cells (see supplementary material S4, supplementary fig. S4.1, Supplementary Material online). This showed that the AHR-deficient HeLa cells expressed about two times higher endogenous *ARNT* mRNA levels than the notoriously AHR-competent human hepatocellular carcinoma cell line HepG2 (Zeiger et al. 2001), hence confirming that ARNT levels were not limiting AHR-mediated responses in these HeLa cells. Therefore, we omitted the cotransfection with ARNT in our main experiments in contrast to the original protocol (Koyano et al. 2005).

The *CYP1A1* Induction Response Is Similar in Human Cells Transfected with Neanderthal and Modern Human AHR

HeLa cells were transfected with an expression construct for either the Altai Neanderthal or the modern human AHR (for details, see above and Materials and Methods). The

transfected HeLa cell population was exposed to a 0–10,000 pM TCDD concentration range, and the dose–response curve for induction of *CYP1A1* mRNA expression was determined (fig. 3). The curves for the cells transfected with the modern human and the Neanderthal AHR almost coincide. Upon fitting the one-site receptor-ligand binding equation to the data (see Materials and Methods, section Data Processing and Statistics), only a small difference in the extrapolated maximal *CYP1A1* induction was observed (Neanderthal AHR attains an 8.3% higher maximum), not in the basal level and the EC$_{50}$ (table 1). This shows that cells transfected with either the Altai Neanderthal or the modern human *AHR* reference cDNA sequence essentially respond similarly to exposure to TCDD.

The G185A SNV in the 5′-UTR of the *AHR* mRNA Affects Reporter Gene Expression

At position 185 of the 5′-UTR (fig. 1) the modern human *AHR* mRNA carries a newly derived A variant (rs7796976 of dbSNP build 153, TopMed data set: A allele frequency = 0.21) which is unique for the human lineage among all presently sequenced primate genomes. The Neanderthal and the Denisovan carry the ancestral G variant (fig. 1), but the
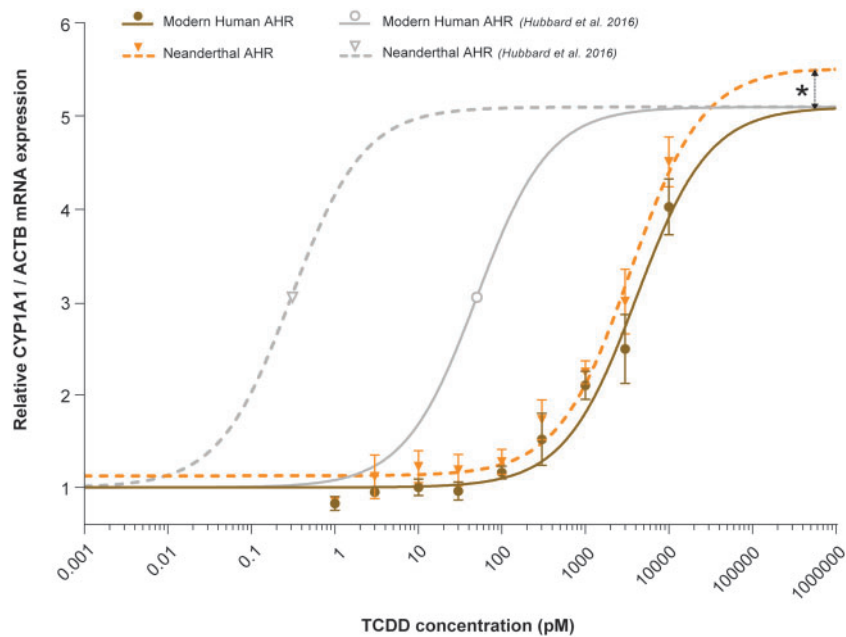
Fig. 3. Dose–response relation observed for *CYP1A1* mRNA induction by TCDD in HeLa human cervix epithelial adenocarcinoma cells transfected with a modern human or Neanderthal AHR expression construct. Each curve is based on two data sets from different HeLa cell batches, and each data set comprised mostly three, or at least two TCDD exposure replicates per data point. Cytochrome P450 1A1 (*CYP1A1*) and β-actin (*ACTB*) mRNA expression were measured in duplicate by qRT-PCR, and *CYP1A1* mRNA expression was normalized to β-actin mRNA expression. The *CYP1A1/ACTB* ratios were subsequently normalized to the basal level for the modern human AHR, that is, this value was set to 1 and all values expressed as a fold value relative to this response level, and plotted against the TCDD concentration in the culture medium during exposure. Error bars indicate the standard error of the mean (SEM). Dose–response curves were generated by fitting the one-site receptor-ligand binding equation to the experimental data (see Materials and Methods, section Data Processing and Statistics), which produced best-fit estimates for the Effective Concentration 50% (EC$_{50}$), and for the basal and maximal values of TCDD-induced *CYP1A1* mRNA expression (table 1). For comparison full-range dose–response curves as reported by Hubbard et al. (2016) are shown in gray based on their observed EC$_{50}$ values and a toxic equivalency factor (TEF) for TCDF = 0.1 to account for the AHR agonist potency difference between TCDF used by them and TCDD (TEF = 1) used in this study (Van den Berg et al. 2006). *The maximal *CYP1A1* induction levels attained by the modern human and Neanderthal AHR were statistically evaluated as different based on the calculated difference in corrected Akaike's information criterion (column ΔAICc in Table 1).

Table 1. Comparison of the Parameters of the Dose–Response Relation for *CYP1A1* mRNA Induction by TCDD in HeLa Cells Transfected with an Expression Construct for Modern Human or Neanderthal AHR.

Curve-Fitting Parameter	Modern Human			Neanderthal				Probability (%) That Parameter Is		Preferred Model Based on ΔAICc
	Best-Fit Value	95% CI		Best-Fit Value	95% CI		ΔAICc	Same	Different	
		From	To		From	To				
Bottom	1.000	0.8428	1.156	1.126	0.9629	1.287	−1.009	62.35	37.65	Same
Top	5.103	4.756	5.453	5.526	5.184	5.871	0.805	40.07	59.93	Different
EC$_{50}$(pM)	4,097	2,837	5,834	3,450	2,443	4,806	−1.811	71.21	28.79	Same

Note.—95% CI, 95% confidence interval for the curve-fitting parameter as reported by GraphPad Prism 8; ΔAICc, difference in corrected Akaike's Information Criterion (AIC) between the simpler model where the parameter is the same for both data sets and the more complex model where the parameter is different for each data set.

anatomically modern human from Ust'-Ishim (45,000 years ago) (Fu et al. 2014) is already heterozygous (see supplementary material S6, Supplementary Material online). Smoking and possessing the G-variant were found to additively increase intestinal permeability in Crohn's inflammatory bowel disease (Prager et al. 2016), demonstrating the functional relevance of this 5′-UTR polymorphism. Moreover, the high-risk 185G variant was found associated with enhanced *AHR* mRNA expression in colon biopsies.

We wondered whether we could confirm the functional effect of this 5′-UTR variant in the context of the Neanderthal and modern human reference *AHR* mRNA sequences studied here. Therefore, we tested the effect of the G185A variation on EGFP reporter gene expression as a proxy for its possible effect on the *AHR* mRNA and/or protein expression. Either the 185G or 185A 5′-UTR sequence was attached to the 5′-end of the EGFP coding region within an EGFP fusion protein expression vector. These constructs were transfected into the
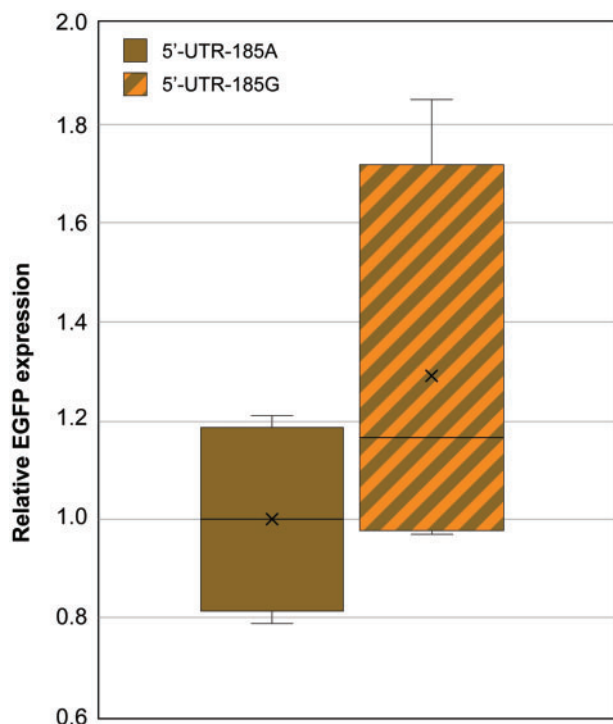
FIG. 4. Effect of the G185A polymorphism (rs7796976) observed in the 5′-UTR of the *AHR* transcript on EGFP expression. A 620-bp 5′-UTR sequence carrying either the 185G or 185A variant was attached to the 5′-side of the EGFP coding region within pcDNA3-EGFP, a cytomegalovirus promoter-driven EGFP fusion protein expression vector, and transfected into AHR-competent HepG2 human liver hepatoma cells. EGFP reporter protein expression directed by the EGFP mRNA carrying the AHR-derived 5′-UTR was normalized to the luciferase expression directed by a cotransfected constitutive luciferase expression construct (see Materials and Methods). Data are from four replicate transfections carried out with two different HepG2 cell batches. To compensate for differences in responsivity between cell batches, all data are presented relative to the mean response observed for the 185A variant. This box and whisker graph is presenting the difference in distribution of the data, with the box showing the 25–75% percentile range, calculated including the median (horizontal line), and mean (x), and the whiskers indicating the minimum and maximum value.

human liver cell line HepG2, which is known to express all factors required for fully functional AHR signal transduction (Zeiger et al. 2001), and hence will be able to reflect the natural function of the *AHR* 5′-UTR. It was observed that the fluorescence signal was approximately 1.3 times higher when the 185G 5′-UTR variant, occurring in the ancient hominins, was inserted before the EGFP reporter (fig. 4). This is consistent with the functional effects of these 5′-UTR variants observed by Prager et al. (2016).

Discussion

As ancient hominin cells cannot be reconstructed to date, the "next best" and feasible option to obtain relevant functional information regarding ancient gene variants is expression in a modern human cellular background. The HeLa human cervical adenoma cell line is particularly suitable to carry out the

comparison between the ancient and modern AHR, as it has been reported as valid for functional testing of *AHR* gene variants (Koyano et al. 2005), because of a low background of endogenous AHR, and nevertheless expressing all essential components, such as ARNT (this study), to support AHR signaling upon transfection with an AHR expression construct. Besides ensuring a homologous cellular background, our study compares the complete ancient hominin *AHR* transcript with the modern human reference, including the 5′- and 3′-UTR with two SNVs in addition to the two SNVs occurring in the coding region, while leaving the original codon usage intact.

Applying these test conditions, we observed that the Neanderthal AHR has a very similar transactivating potency as compared with the modern human AHR: no significant difference in basal level and EC_{50} for induction of *CYP1A1* mRNA by TCDD, and only a small difference in the maximal induction level (8.3% higher), found at very high TCDD concentrations, above 3 nM of TCDD toxic equivalents (TEQ). It is debatable, however, whether such high on-target concentrations are still relevant for real-life exposure levels. Significant variation among modern humans has been observed regarding the dissociation constant (K_d) for the binding of TCDD to the AHR, respectively, the EC50 for downstream AHR-controlled effects, such as CYP1A1 induction (Roberts et al. 1990; Harper et al. 2002; Silkworth et al. 2005; Van den Berg et al. 2006; Forgacs et al. 2013). The cited references report a 0.087–18 nM range. The EC_{50} for CYP1A1 mRNA induction observed by us (4.1 nM) and by Hubbard et al. (2016) (0.5 nM 2,3,7,8-tetrachlorodibenzofuran [TCDF], equivalent to 0.05 nM TCDD) appear to lay in the upper and just below the lower part of this range, respectively.

These results also apply to the Denisovan because its *AHR* mRNA sequence is identical to the tested Altai-Neanderthal sequence (fig. 1), and are likely to be representative for the Vindija-Neanderthal as well. Its *AHR* mRNA has a deviation from the Altai sequence at two UTR positions at the most, dependent on the allele considered and the unknown haplotype coupling of these differences, which have not been reported in modern humans to be of any physiological relevance (dbSNP, build 153).

The Effect of the Ancient 185G 5′-UTR Variant on Gene Expression Is Similar as Reported in Modern Humans

The ancestral 185G *AHR* 5′-UTR variant found in the ancient hominins studied (fig. 1, supplementary fig. S6, Supplementary Material online) is still abundant in the present-day human population at a 79% frequency (dbSNP build 153, rs7796976), and was found associated with an epithelial barrier defect in smokers with Crohn's disease and higher *AHR* mRNA expression (Prager et al. 2016). The increased EGFP reporter protein expression observed to be conferred by the 185G 5′-UTR variant as compared with the 185A variant (fig. 4) is consistent with these findings, and provides evidence for the functional significance of the 185G 5′-UTR variant observed in the ancient *AHR* sequences.

Its effect on protein expression is likely due to an effect on translation efficiency or a posttranscriptional effect on *AHR* mRNA levels.

Other Genes Playing a Role in Deactivation of Environmental Toxins

The new results presented here imply that the Ala381Val mutation that became fixed in the modern human lineage might be less relevant for the evolution of Ah receptor-controlled detoxification than suggested by Hubbard et al. (2016). Instead, many more genes have been shown to be involved in detoxification of dioxin-like toxicants (Moorthy et al. 2015), which appeared to be predominantly in the ancestral, protective state in ancient hominins, whereas less protective variants appear in the modern human lineage (Aarts et al. 2016).

Limited Impact of the Ala381Val Substitution in the Modern Human Lineage

In a human cellular background, no significant difference in EC_{50} for *CYP1A1* induction was found between the modern Val381 and ancient hominin Ala381 AHR protein variants, suggesting no or only a small difference in AHR sensitivity to the prototypical agonist TCDD. At first sight, this may seem at odds with previous comparative studies reporting a higher affinity for TCDD of "Ala-type" (mouse Ala375/rat Ala379) as compared with "Val-type" (human Val381/mouse Val375) AHRs. This amino acid difference mostly results in EC_{50} values around ten times lower for AHR-mediated effects of the Ala-type receptors (Ema, Matsushita, et al. 1994; Okey et al. 2005; Silkworth et al. 2005; Connor and Aylward 2006; Flaveny et al. 2009; Budinsky et al. 2010). The Neanderthal receptor, the first "humanized" Ala-type receptor ever studied, with a reported 150- to 1,000-fold difference in EC_{50} for *CYP1A1* induction when compared with the modern human Val-type AHR in rat cells (Hubbard et al. 2016) seems to be an extreme case of this tendency. How to explain this discrepancy? A review of the previously published experimental and molecular modeling literature on the difference between the two types of AHR revealed extensive argumentation supporting our observations. Below these arguments have been categorized according to 1) the role of the variation in AHR protein size, 2) effects of species-specific and reciprocal allosteric interactions within the AHR complex, 3) methodological limitations, and 4) evidence from molecular modeling.

First of all, the best-fit EC_{50} estimate observed here in a human cellular background for the Neanderthal Ala-type AHR was still slightly lower than the best-fit value found with the modern human Val-type AHR, and may, in fact, be up to approximately two times lower based on the calculated 95% confidence intervals (table 1). Therefore, although we observed a smaller than ten times EC_{50} difference between the ancient hominin Ala381 and modern human Val381 AHR types, this result is still qualitatively consistent with the previously reported difference. But even a close similarity in EC_{50} may, on second thought, not be so surprising in view of the following theoretical considerations and reported observations:

Role of AHR Protein Length

The initial comparative studies on the human AHR, and the AHR from dioxin-sensitive and -resistant mouse and rat strains showed that the observed length variation of the AHR polypeptide (albeit in opposite directions for mouse and rat, and only for limited toxic endpoints [Okey et al. 2005] for the rat) has an equally important impact on its functionality as the Ala>Val mutation (Ala379Val never investigated in rat) (Ema, Ohe, et al. 1994; Pohjanvirta et al. 1998).

Effects of Species-Specific and Reciprocal Allosteric Interactions within the AHR Complex

The Ala>Val variation has been extensively studied in cellular backgrounds compatible with the Ala-type AHR, for instance, rodent (Okey et al. 1989; Poland and Glover 1990; Hubbard et al. 2016) and monkey (Ema, Ohe, et al. 1994; Silkworth et al. 2005; Connor and Aylward 2006; Hubbard et al. 2016), but to the best of our knowledge, never the other way around. In particular lacking are studies of an Ala-type receptor in Val-type AHR-compatible (i.e., human) cells, since before the discovery that ancient hominins still carried the ancestral Ala381 variant in a human-like polypeptide context there was no logical incentive to do so. Our study therefore seems to be the first of this type.

The affinity for a ligand is obviously an intrinsic property of a receptor, primarily determined by the stereochemical interaction characteristics of a receptor-ligand pair. However, evidence is accumulating, for the androgen receptor (Baek et al. 2006; Claessens et al. 2017; Senapati et al. 2020) and other nuclear receptors (NRs) (Billas and Moras 2013; De Vera et al. 2017), supporting the view that in vivoin vivo functioning of NRs and other ligand-activated transcription factors such as the AHR involves extensive communication between functional domains. This applies both to functional domains within a receptor and to domains in other components of the receptor complex, such as the dimerization partner, chaperones, and cofactors. These interdomain interactions may be modulated by the interaction with various ligands and variable DNA response element configurations and nucleotide sequences. Therefore, the ultimate transactivation outcome will depend on the integral result of all interactions and allosteric effects that may occur between ligands, protein domains, and response element nucleotides within the ultimate DNA-bound receptor complex taking part in assembly of the transcription machinery in the upstream gene regulatory region, and of such interactions during the steps leading up to it. Most importantly, the above-mentioned interactions and allosteric effects are considered to act in a reciprocal way. Seok et al. (2017) determined the crystal structure of a mouse AHR–human ARNT heterodimer in complex with a DRE and concluded for the specific case of the AHR: ". . . the complex dimerization and interdomain interfaces remotely control target DNA binding and the induction of AHR activity, which, . . ., suggests an allosteric structural pathway for mediating changes from the ligand-binding PAS-B domain to the DNA-reading head, or reciprocally, from the DNA-reading head to

the ligand-binding domain or farther to the transactivation domain" (Seok et al. 2017, p. 5434).

Zhang et al. (2008) found that the potency of prototypical AHR agonists, including TCDD used here and TCDF used by Hubbard et al. (2016), to induce transactivation in a two-hybrid AHR-coactivator interaction assay was dependent on the species and tissue origin of the cell type in which the AHR–coactivator interaction was studied. Although this study did not take into account the possible effect of ARNT on the AhR–coactivator interaction, it clearly showed the potential of cell-specific factors such as coactivators to modulate AHR agonist potency.

Furthermore, domain swapping experiments between the guinea pig and mouse AHR by Henry and Gasiewicz (2008) showed that the C-terminal part of the receptor, containing the transactivation domain, and not the ligand binding domain (LBD) itself, determines whether 3′-methoxy-4′-nitroflavone will act as an AHR agonist or not (and even turn into an antagonist) (Henry and Gasiewicz 2008). This concept is also supported by a range of experimental observations showing that binding of an activated (nuclear) receptor to its response element via the DNA binding domain induces allosteric effects in other domains which may affect the dimerization interface, coregulator recruitment or even ligand potency. De Vera et al. (2017), for example, reported for the case of the PPARγ–RXRα heterodimer: "DNA binding propagates a conformational change in PPARγ–RXRα, stabilizes the receptor LBD dimer interface, and impacts ligand potency and cooperativity in NR coactivator recruitment" (De Vera et al. 2017, p. 1506). Similarly, for the androgen receptor there are reports of this phenomenon (Zhou et al. 1995; Langley et al. 1998; He et al. 2000; Helsen et al. 2012; Meijer et al. 2019), as there are for other NRs (Shao et al. 1998; Gee et al. 1999; Helsen and Claessens 2014; De Vera et al. 2017; Meijer et al. 2019).

Furthermore, the mouse AHR protein was shown to comprise, in addition to several synergistic stimulatory subdomains, an inhibitory subdomain in its C-terminal *trans*-activating domain which interacts with heat-shock protein HSP90 and functions in a species-, cell type-, and promoter-specific way (Whitelaw et al. 1994; Ma et al. 1995).

This reciprocal allosteric cross-talk concept opens up an avenue along which changes in interfaces with species- (or cell-)specific dimerization partners, chaperones, coactivators or other cofactors interacting with the AHR during signal transduction may have an effect on the conformation of the ligand or DNA binding domain, and thereby affect the ligand or DNA binding affinity of the AHR complex as it occurs in vivo, and consequently, influence the EC_{50} values of AHR agonists observed for AHR-controlled responses in a species- (or cell-) specific way.

Methodological Limitations

As a matter of fact, due to technical limitations AHR ligand and DNA binding studies have necessarily been incomprehensive regarding the above-mentioned relevant interactions, for example, using in vitro translated AHR variant and/

or ARNT protein preparations lacking other relevant cell factors (Pandini et al. 2007), or ARNT (Chiaro et al. 2008; Hubbard et al. 2015), cytosol (Ema, Ohe, et al. 1994; Flaveny et al. 2009) or response element DNA (Bank et al. 1992; Singh et al. 1996; Hubbard et al. 2015) of heterologous origin. In view of the existence of extensive (allosteric) interactions, these limitations may have contributed to the apparent divergence of previous TCDD affinity and DNA binding measurements from the results reported here.

Pandini et al. (2007) reported an anomaly observed with the Ala375Val mutation in the mouse AHR. Although they did not observe any TCDD binding by Val375 AHR, this variant appeared to still have 42% of the DNA binding capacity of the Ala375 variant; it required changing Ala375 to the much bulkier leucine (Leu) to completely prevent DNA binding, suggesting that the effect of Val375 may not, or only partially result from steric hindrance (see their table 4). The authors hypothesize a number of technical causes which are plausible indeed, but quantitatively leave a gap. Therefore we propose a possible additional biological explanation, which would be consistent with our observations: The [³H]TCDD binding assay reaction was carried out with in vitro translated AHR only, whereas the DNA binding assay was carried out in the presence of ARNT. A possible interpretation of their observation would be that the Val375 AHR complex was in a different conformation in the presence of ARNT, causing a proportional difference between the ligand-induced DNA binding by the ultimate DNA-bound complex at chemical equilibrium and, on the other hand, the level of ligand binding at equilibrium to the AHR in isolation. These experimental data are therefore consistent with our view that the "penetrance" of the Ala>Val variation is dependent on the ultimate composition, and hence the conformation, of the ligand-activated AHR/ARNT/cofactor/DNA complex formed, which is obviously species-dependent.

Evidence from Molecular Modeling

Bonati et al. (2017) recognized that, for that matter, analogous limitations apply to molecular modeling and ligand docking studies with the AHR: "To reach a better predictive ability, in silico modeling should move toward a molecular description of the entire process by which ligands differentially affect the AhR activation, stimulate AhR transformation and DNA binding, and activate AhR-dependent gene expression" (Bonati et al. 2017, p. 45).

In addition to the possibility that cell-specific allosteric effects play a role, a range of molecular modeling outcomes and experimental observations are arguing against the perception that the in vivo effect of the Ala>Val substitution is mainly the consequence of its effect on ligand binding:

A recent molecular docking simulation using a 3D homology model of the basic–helix–loop–helix (bHLH) - Per–Arnt–Sim (PAS) ligand binding and dimerization domain from the murine AHR (mAHR), which followed a new approach taking into account receptor flexibility, revealed that the per-residue contribution of Ala375 in the mAHR to the free energy

decrease (ΔG_{bind}) of TCDD binding is minimal (Giani Tagliabue et al. 2019), essentially implying no role for Ala375 in stabilizing TCDD in the ligand binding pocket of the mAHR. This implies that Ala375 binding does not explain the higher affinity for TCDD of the mouse Ala-type AHR, or, by analogy, the very much higher affinity and potency in rat cells in case of the Neanderthal AHR (Hubbard et al. 2016) as compared with the Val-type AHRs, although this does not exclude that steric hindrance would play a certain role. The somewhat, but not much more bulky Val residue (with an isopropyl instead of a methyl side chain) may indeed block TCDD to a certain extent from entering the ligand binding pocket. Against steric hindrance by the Val side chain argues, however, that Ema, Ohe, et al. (1994) observed no effect on TCDD binding of changing Val381 in the human AHR to Leu (with an even more bulky side chain) or to Gly (no side-chain at all). In contrast, it required changing the nonpolar Val381 into the dissimilar polar amino acid aspartic acid (Asp) to effectively abolish TCDD binding, which would be consistent with the nature of the interaction with another amino acid side chain being the crucial issue (Ema, Ohe, et al. 1994).

Similarly, A361 and A375 of the mouse AHR are on adjacent strands of the β-sheet that is modeled to form one side of the ligand cavity (Procopio et al. 2002). Changing Ala361 to the larger but still nonpolar amino acids Val or Leu completely eliminated TCDD binding and TCDD-induced DRE binding. However, changing the adjacent Ala362 into Leu had much less effect, especially on DNA binding, which was still 69% of the wild-type level (Henry and Gasiewicz 2008, calculated based on their figure 2a). This, again, may indicate that another mechanism than steric hindrance may play a role in causing the effects of these mutations at position 361, 362, and (by analogy) 375 of the mouse AHR LBD.

Furthermore, the mere fact that the amino acid at position 381 is located near the end of the human AHR amino acid chain making up the LBD (amino acids 247–391) (Bisson et al. 2009) makes it more likely, regardless of the way of polypeptide chain folding, to engage in interactions outside the LBD, and thus to have an indirect, allosteric effect on agonist potency.

Altogether these experimental, 3D modeling and molecular docking data, and methodological limitations provide substantial evidence that the discrepancy between the experimental results described here and previous studies, if perceived as contradictory in the first place, can be explained by 1) allosteric effects due to heterologous AHR dimerization partners, chaperones, coactivators or other protein factors interacting with the AHR (complex), for example, when expressed in cells from a heterologous species; and 2) the use of in vitro in vitro test conditions lacking some in vivo in vivo AHR complex constituents. Finally, in view of the obvious difference in sensitivity to TCDD between the ancient hominin AHR with Ala381 (observed in this study to be comparable to the modern human Val-type AHR) and the rodent Ala-type AHRs (reported in many in vitro in vitro and in vivo in vivo studies to be approximately ten times more responsive to TCDD than the human Val-type AHR; see above), it cannot be excluded, that the many existing species differences in

amino acid sequence other than the one at position 381 (see supplementary material S9, Supplementary Material online) are playing a role. Most importantly, our results imply a caveat against the use of cellular models derived from heterologous species in gene product expression and characterization studies.

Several Evolutionary Mechanisms May Explain Val381 Fixation

As our results imply no difference between the AHR from Neanderthals and modern humans with regard to activation by the standard AHR agonist TCDD, the question arises why the Val381 variant has reached fixation in the modern human lineage. It is possible that there is still a significant physiological difference between these AHR variants toward other agonists than dioxin-like compounds, or AHR antagonists, such as bioactive plant food components (Denison et al. 2011), or endogenous AHR ligands such as tryptophan photooxidation products that need to be balanced at optimal levels (Wincent et al. 2012). Theoretically, we cannot completely exclude that this also pertains to TCDF used by Hubbard et al. (2016). If so, this may contribute to the discrepancy with our study, but actually, this is very unlikely, because TCDD and TCDF are both generally recognized as very similar full AHR agonists (Kopec et al. 2010) that have, to the best of our knowledge, never been reported to display divergent toxicity before. Besides that, it would not argue in any way the physiological relevance of the diverging results reported here for the prototype AHR agonist TCDD.

Altogether, the Val381 AHR variant may still confer a fitness advantage related to such alternative AHR-active compounds which could have driven the fixation process. Two other possible mechanisms that do not involve positive genetic selection of the AHR Val381 variant itself are conceivable: 1) fixation by random genetic drift, which could have been enhanced by the small size of early modern human populations (Whitlock 2000; Meyer et al. 2012; Prüfer et al. 2017); and 2) positive selection on a gene that is genetically tightly linked to the AHR locus. A candidate could be the genomic region reported to be ranking at position 21 in terms of selective sweep strength in the modern human lineage, which is about 1 Mb from the AHR locus (chromosome 7: 18339385–18546684 in genome assembly GRCh38/hg38; see table S37 in Green et al. [2010]). This region contains one gene, HDAC9, encoding histone deacetylase 9. Histone deacetylation provides a tag for epigenetic repression and plays an important role in transcriptional regulation, cell cycle progression, and developmental events (Méjat et al. 2005; Delcuve et al. 2012). In view of the close vicinity of the HDAC9 gene it is possible that, early in the modern human lineage, the AHR Val381 variant was driven to fixation because of the lack of recombination between the newly arisen AHR Var381 variant and the selective sweep region containing HDAC9.

No Major Role of AHR in Neandertal Detoxification Capacity of Smoke-Related Toxic Compounds, Consistent with Our Previous Study

As far as the deep history of fire use is concerned, our previous study (Aarts et al. 2016) was inconclusive regarding the use of fire by Neanderthals and Denisovans, as the high prevalence of low risk, but mostly ancestral detoxification gene variants in their genome did not allow conclusions regarding positive genetic selection. Modern humans, on the other hand, appeared to be evolving toward decreased detoxification efficacy in spite of their stronger dependence on fire use. The results presented here do not change this assessment, and are strongly at odds with suggestions that a mutation in the AHR may have given modern humans an evolutionary advantage over Neanderthals in adapting to smoke exposure.

Future Directions

With a view to future research into the physiological properties of ancient hominin gene variants it appears crucial to reconstruct their expression conditions as faithfully as possible, especially the cell type used, which should be preferentially of human origin. We showed here that there is no essential difference between the ancient and modern AHR regarding activation by the toxic AHR agonist TCDD also occurring at low levels in smoke. It remains to be seen, however, whether this indifference extrapolates to all classes of AHR-active compounds, including major smoke toxins such as PAHs. Such studies, in particular of dietary and endogenous AHR agonists will be crucial to understand the full biological impact of the observed ancient AHR variations.

Materials and Methods

Detailed Ancient AHR Variant Testing Strategy

UTRs of a gene transcript may contain functional elements embedded in the primary sequence, or hairpins or other secondary structures serving as protein or micro-RNA binding sites that play a role in translation initiation and regulation, mRNA stability, transport from the nucleus, or cellular localization (Hinnebusch et al. 2016; Mayr 2017). Specifically for the AHR mRNA a 5′-UTR variant has been described in the modern human (rs7796976) that increases AHR mRNA expression (Prager et al. 2016) and also occurs in the ancient hominin AHR sequences studied here (position 185 in fig. 1). For the AHR 3′-UTR, a binding site for micro-RNA 124 was recently described (Liu et al. 2018) involved in regulating its expression level as well. Furthermore, changing the natural codons may affect the protein translation efficiency and the ultimate expression level as compared with the natural mRNA sequence (Brule and Grayhack 2017). It may therefore produce artifacts in the functional analysis of the AHR variants and distort their comparison when applied to amino acids at positions where they are different (Ala, Val, Arg, Lys). Therefore, we tested the complete and original AHR mRNA sequence, including the 5′- and 3′-UTR, without mammalian codon optimization.

Synthesis of Modern Human and Neanderthal AHR cDNA Sequences

The modern human AHR variant tested (fig. 1) was the Ensembl AHR transcript AHR-201 (ENST00000242057.8) which is based on expert-curated sequence information and has been assigned the "gold" status, implying that this transcript is identical between Ensembl automated annotation and VEGA/Havana manual curation (Cunningham et al. 2019; EMBI-EBI 2020). An extra T deoxynucleotide was added to its 3′-terminus based on RefSeq AHR mRNA record NM_001621.4, which is also manually curated (NCBI 2017).

The Altai-Neanderthal AHR mRNA sequence carrying four single nucleotide changes as compared with the modern human reference was selected to be tested (see Results). It was retrieved from the VCF data files published (Prüfer et al. 2014, 2017) as described in supplementary material S10, Supplementary Material online. A synthetic double-stranded copy DNA (cDNA) of the modern human AHR mRNA reference sequence (supplementary material S2, Supplementary Material online) and of the Altai-Neanderthal derivative generated by site-directed mutagenesis (supplementary material S3, Supplementary Material online) were purchased from BaseClear (Leiden, the Netherlands). Both synthetic sequences were verified to be 100% correct by Sanger sequencing.

Construction and Preparation of AHR Expression Constructs

The synthetic modern human and Altai-Neanderthal cDNA sequences were produced including 5′-terminal PstI and 3′-terminal XhoI restriction sites which were used to insert them into the expression vector pcDNA3.1/Zeo(+) (Invitrogen, Fisher Scientific, Landsmeer, the Netherlands) using standard recombinant DNA techniques (Sambrook and Russell 2001). These expression constructs were propagated in Escherichia coli DH5α and plasmid DNA was isolated using the E.Z.N.A. Endo-Free Plasmid DNA Mini Kit II (Omega bio-tek, VWR, Breda, the Netherlands) to obtain endotoxin-free plasmid DNA suitable for transfection. For unknown reasons, specifically for the Neanderthal variant plasmid, the best yield was obtained when starting from a single, freshly grown bacterial colony and doubling the normal ampicillin level during propagation to 200 μg/ml. The identity of the obtained plasmid preparations was confirmed again by Sanger sequencing around the Ala381Val variation site (fig. 1, C/T at position 1785) using the primers listed in supplementary material S8, Supplementary Material online.

Human Cell Culture and Transfection

The human cervix epithelial adenocarcinoma cell line HeLa was purchased from the American Type Culture Collection, and the liver carcinoma cell line HepG2 from the European Collection of Authenticated Cell Cultures (Sigma-Aldrich Chemie N.V., Zwijndrecht, the Netherlands). General cell culture supplies were from Gibco (Life Technologies Europe B.V., Bleiswijk, the Netherlands) if not indicated otherwise: HeLa cells were cultured in Dulbecco's Modified Eagle Medium (DMEM) + 4.5 g/l D-glucose + L-glutamine + 25 mm

HEPES (4-(2-hydroxyethyl)-1-piperazineethanesulfonic acid) without pyruvate (42430-025) to which MEM nonessential amino acids (11140-035) were added and 10% fetal bovine serum (Sigma, F7524, Sigma-Aldrich Chemie N.V). HepG2 cells were cultured in Eagle's Minimum Essential Medium (EMEM) + Earle's salts without L-glutamine (21090-022) to which MEM nonessential amino acids (11140-035) were added and 10% fetal bovine serum (American Type Culture Collection, ATCC 30-2020, LGC Standards GmbH, Wesel, Germany).

For transfections, HeLa and HepG2 cells were seeded at approximately 80% density in 96-well plates (Greiner Bio-One 655180). HeLa cells were transfected using the *Trans*IT-HeLaMONSTER Transfection Kit (MIR 2904) and HepG2 cells with *Trans*IT-LT1 Transfection Reagent (MIR 2304) applying the standard protocols (both from Mirus Bio LLC, Sopachem B.V., Ochten, the Netherlands).

Exposure of Transfected HeLa Cells

Forty to forty-four hours after transfection, three replicate wells with HeLa cells were exposed per concentration of TCDD to be tested by adding an equal volume of medium containing twice the final concentration. TCDD (purity 98%, Schmidt B.V., Amsterdam, the Netherlands) was dissolved in dimethyl sulfoxide (spectrophotometric grade, purity 99,9%, Acros Organics 167852500, Fisher Scientific) as a vehicle to add it to culture medium (final concentration 0.4% v/v dimethyl sulfoxide). The concentration of the TCDD parent solution used to prepare the dilution series was calibrated by gas chromatography–mass spectrometry analysis. As TCDF used by Hubbard et al. (2016), TCDD is also a full AHR agonist with a ten times greater potency to activate the AHR (WHO-TEF of TCDF is 0.1 [Van den Berg et al. 2006]).

AHR 5′-UTR—EGFP Reporter Gene Fusion Constructs

The modern human reference and ancient *AHR* mRNA sequences differ consistently at position 185 of the 5′-UTR (numbering of fig. 1; r.-459g>a using HGVS nomenclature [den Dunnen et al. 2016] based on translation start). Both 5′-UTR variants were generated by PCR using Phusion High-Fidelity DNA polymerase (New England Biolabs M0530) and, as a template, the full-length *AHR* cDNA clone SC119159 purchased from Origene (delivered in vector pCMV6-XL4; distributor Acris Antibodies GmbH, Herford, Germany). A segment from this construct (bp 918–1,612) carrying the complete SC119159 5′-UTR (185A-variant) and an upstream *Eco*RI restriction site was amplified using primers pCMV6-XL4_918-937 and AHR_ENST643-630_*Xho*I, the latter including a 3′-terminal *Xho*I restriction site and a 6-bp clamp (sequence details and annealing temperature in supplementary material S8, Supplementary Material online). The ancient G-variant of this segment was generated by overlap extension PCR (Heckman and Pease 2007). The upper mutated overlap segment (bp 918–1,169 of SC119159) was generated using the primer pair pCMV6-XL4_918-937 and AHR_ENST200-170_185G_rev, and the lower mutated overlap segment (bp 1,142–1,612) with primer pair AHR_ENST173-

203_185G_fwd and AHR_ENST643-630_*Xho*I. Before fusion PCR, both segments were column-purified using the GeneJET PCR Purification Kit K0702 (Thermo Scientific, K0702, VWR, Breda, the Netherlands). The fusion reaction of these segments contained 100 pg of the short (252 bp) and 200 pg of the long fragment (471 bp; overlapping 28 bp with the shorter segment), 10 μM of primers pCMV6-XL4_918-937 and AHR_ENST643-630_*Xho*I, 10 mM dNTPs, 1× Phusion HF Buffer, and 1 unit of Phusion DNA polymerase in 50 μl reaction volume. After initial denaturation at 98 °C for 30 s this reaction mixture was subjected to five cycles of 10 s 98 °C, 3 min 55 °C, and 30 s 72 °C, followed by a finishing incubation at 72 °C for 5 min. The undetectable amount of fusion product formed was column-purified using the GeneJET PCR Purification Kit and reamplified using the outer primers pCMV6-XL4_918-937 and AHR_ENST643-630_*Xho*I. The generated fusion product (707 bp) was column-purified, digested with *Eco*RI and *Xho*I, again column-purified, and then ligated applying standard cloning techniques into *Eco*RI- and *Xho*I-digested and subsequently gel-purified pcDNA3-EGFP, a cytomegalovirus immediate-early promoter/enhancer-controlled EGFP fusion protein expression vector (gift from Doug Golenbock; RRID: Addgene_13031; available from Addgene, Cambridge, MA). The resulting construct was propagated in *E. coli* DH5α according to standard methods (Sambrook and Russell 2001) and purified for transfection of human HepG2 cells using the E.Z.N.A. Endo-free Plasmid DNA Mini Kit II (Omega Bio-tek D6950-01, VWR, Breda, the Netherlands). The A- or G-variant type and insert sequence of the final plasmid preparations was confirmed to be 100% correct by Sanger sequencing. An aligned overview of the vector template, primers, overlap segments, overlap extension product, vector insert, and *AHR* 5′-UTR aligned to the human *AHR* mRNA reference sequence is available in supplementary material S7, Supplementary Material online.

Quantification of Protein Expression Directed by the AHR 5′-UTR-EGFP Fusion mRNA

The 185A or 185G *AHR* 5′-UTR-EGFP fusion mRNA constructs were cotransfected (ratio 1:1) with pBV-Luc (He et al. 1999) (a gift from Bert Vogelstein; RRID: Addgene_16539; available from Addgene), carrying a firefly luciferase coding sequence under control of a minimal promoter, into HepG2 cells known to feature natural AHR expression and signaling (Zeiger et al. 2001). EGFP expression was measured using a 96-well fluorescence plate reader (Tecan Infinite M200 PRO) using the standard settings for EGFP quantification. EGFP expression was normalized for transfection efficiency based on the luciferase expression conferred by the cotransfected pBV-Luc plasmid, which was quantified using flash kinetics and a double injector automated plate reader (Glomax 96 E6521, Promega Corporation, Madison, WI) to subsequently inject luciferase substrate (Flash Mix according to Boerboom et al. [2006]) and 0.2 M sodium hydroxide stop reagent.

Measuring mRNA Expression Levels Using Quantitative PCR

Dose–response curves for the induction of *CYP1A1* mRNA expression by TCDD exposure were determined after 24 h of exposure using quantitative reverse transcription PCR (qRT-PCR). *AHR* mRNA to assess the level of overexpression, zeocin resistance gene (ZEO) expression to quantify transfection efficiency, as well as β-actin (*ACTB*) mRNA expression levels were determined in sample aliquots measured in parallel. All qRT-PCR data, including background *AHR* and *ARNT* mRNA levels measured in HeLa and HepG2 cells, were normalized for differences in cDNA input based on *ACTB* mRNA expression. Harvesting of cells from 96-well cell culture plates and qRT-PCR was carried out using the Ambion Power SYBR Green Cells-to-C_T Kit (Thermofisher Scientific 4402954). Alternatively, for small-scale experiments and nontransfected HeLa and HepG2 cells, total RNA was isolated using TRIzol reagent (Invitrogen, Fisher Scientific), reverse transcribed into cDNA using the iScript cDNA Synthesis Kit, and quantitative PCR was carried out using IQ SYBR Green Supermix (both from Bio-Rad Laboratories B.V., Veenendaal, the Netherlands). All primers and annealing temperatures used are listed in supplementary material S8, Supplementary Material online. Melt-curve analysis was performed to assure a single PCR product of the expected melting temperature. A Bio-Rad CFX Connect thermocycler was used throughout.

Data Processing and Statistics

Dose–response data were analyzed using GraphPad Prism 8 software to determine the best fit to the data of the equation Y = Bottom + [X * (Top-Bottom)/(EC_{50} + X)], describing the relation between the response (Y = *CYP1A1* mRNA level) and the agonist concentration (X = concentration TCDD) for a receptor with one ligand binding site such as the AHR. The output includes best estimates for the basal (Bottom) and maximal *CYP1A1* induction level (Top), and for the agonist concentration inducing a half maximal response (EC_{50}) as well as a 95% confidence interval for these curve fitting parameters. The output values of these parameters for the modern human and Neanderthal AHR were statistically evaluated as different or not based on the difference in corrected Akaike's information criterion values (ΔAICc) as calculated by GraphPad Prism 8 (GraphPad Software 2020).

Supplementary Material

Supplementary data are available at *Molecular Biology and Evolution* online.

Acknowledgments

References

Aarts JM, Alink GM, Scherjon F, MacDonald K, Smith AC, Nijveen H, Roebroeks W. 2016. Fire usage and ancient hominin detoxification genes: protective ancestral variants dominate while additional derived risk variants appear in modern humans. *PLoS One* 11(9):e0161102.

Baek SH, Ohgi KA, Nelson CA, Welsbie D, Chen C, Sawyers CL, Rose DW, Rosenfeld MG. 2006. Ligand-specific allosteric regulation of coactivator functions of androgen receptor in prostate cancer cells. *Proc Natl Acad Sci U S A.* 103(9):3100–3105.

Bank PA, Yao EF, Phelps CL, Harper PA, Denison MS. 1992. Species-specific binding of transformed Ah receptor to a dioxin responsive transcriptional enhancer. *Eur J Pharmacol Environ Toxicol Pharmacol.* 228(2–3):85–94.

Billas I, Moras D. 2013. Allosteric controls of nuclear receptor function in the regulation of transcription. *J Mol Biol.* 425(13):2317–2329.

Bisson WH, Koch DC, O'Donnell EF, Khalil SM, Kerkvliet NI, Tanguay RL, Abagyan R, Kolluri SK. 2009. Modeling of the aryl hydrocarbon receptor (AhR) ligand binding domain and its utility in virtual ligand screening to predict new AhR ligands. *J Med Chem.* 52(18):5635–5641.

Boerboom A-M, Vermeulen M, van der Woude H, Bremer BI, Lee-Hilz YY, Kampman E, van Bladeren PJ, Rietjens IMCM, Aarts J. 2006. Newly constructed stable reporter cell lines for mechanistic studies on electrophile-responsive element-mediated gene expression reveal a role for flavonoid planarity. *Biochem Pharmacol.* 72(2):217–226.

Bonati L, Corrada D, Giani Tagliabue S, Motta S. 2017. Molecular modeling of the AhR structure and interactions can shed light on ligand-dependent activation and transformation mechanisms. *Curr Opin Toxicol.* 2:42–49.

Brule CE, Grayhack EJ. 2017. Synonymous Codons: choose Wisely for Expression. *Trends Genet.* 33(4):283–297.

Budinsky RA, LeCluyse EL, Ferguson SS, Rowlands JC, Simon T. 2010. Human and rat primary hepatocyte CYP1A1 and 1A2 induction with 2,3,7,8-tetrachlorodibenzo-p-dioxin, 2,3,7,8-tetrachlorodibenzofuran, and 2,3,4,7,8-pentachlorodibenzofuran. *Toxicol Sci.* 118(1):224–235.

Carmody RN, Wrangham RW. 2009. The energetic significance of cooking. *J Hum Evol.* 57(4):379–391.

Chatterjee S, Pal JK. 2009. Role of 5′- and 3′-untranslated regions of mRNAs in human diseases. *Biol Cell.* 101(5):251–262.

Chiaro CR, Morales JL, Prabhu KS, Perdew GH. 2008. Leukotriene A4 metabolites are endogenous ligands for the Ah receptor. *Biochemistry* 47(32):8445–8455.

Claessens F, Joniau S, Helsen C. 2017. Comparing the rules of engagement of androgen and glucocorticoid receptors. *Cell Mol Life Sci.* 74(12):2217–2228.

Connor KT, Aylward LL. 2006. Human response to dioxin: aryl hydrocarbon receptor (AhR) molecular structure, function, and dose-response data for enzyme induction indicate an impaired human AhR. *J Toxicol Environ Health B Crit Rev.* 9(2):147–171.

Corchero J, Pimprale S, Kimura S, Gonzalez FJ. 2001. Organization of the CYP1A cluster on human chromosome 15: implications for gene regulation. *Pharmacogenetics* 11(1):1–6.

Cunningham F, Achuthan P, Akanni W, Allen J, Amode MR, Armean IM, Bennett R, Bhai J, Billis K, Boddu S, et al. 2019. Ensembl 2019. *Nucleic Acids Res.* 47(D1):D745–D751.

De Vera IMS, Zheng J, Novick S, Shang J, Hughes TS, Brust R, Munoz-Tello P, Gardner WJ, Marciano DP, Kong X, et al. 2017. Synergistic regulation of coregulator/nuclear receptor interaction by ligand and DNA. *Structure* 25(10):1506–1518.e4.

Dechanet C, Anahory T, Mathieu Daude JC, Quantin X, Reyftmann L, Hamamah S, Hedon B, Dechaud H. 2011. Effects of cigarette smoking on reproduction. *Hum Reprod Update.* 17(1):76–95.

Delcuve GP, Khan DH, Davie JR. 2012. Roles of histone deacetylases in epigenetic regulation: emerging paradigms from studies with inhibitors. *Clin Epigenetics*. 4(1):5.

DeMarini DM. 2004. Genotoxicity of tobacco smoke and tobacco smoke condensate: a review. *Mutat Res*. 567(2–3):447–474.

Den Dunnen JT, Dalgleish R, Maglott DR, Hart RK, Greenblatt MS, McGowan-Jordan J, Roux A-F, Smith T, Antonarakis SE, Taschner PEM, on behalf of the Human Genome Variation Society (HGVS), the Human Variome Project (HVP), and the Human Genome Organisation (HUGO). 2016. HGVS recommendations for the description of sequence variants: 2016 Update. *Hum Mutat*. 37(6):564–569.

Denison MS, Soshilov AA, He G, DeGroot DE, Zhao B. 2011. Exactly the same but different: promiscuity and diversity in the molecular mechanisms of action of the aryl hydrocarbon (dioxin) receptor. *Toxicol Sci*. 124(1):1–22.

Divi RL, Einem Lindeman TL, Shockley ME, Keshava C, Weston A, Poirier MC. 2014. Correlation between CYP1A1 transcript, protein level, enzyme activity and DNA adduct formation in normal human mammary epithelial cell strains exposed to benzo[a]pyrene. *Mutagenesis* 29(6):409–417.

Ema M, Matsushita N, Sogawa K, Ariyama T, Inazawa J, Nemoto T, Ota M, Oshimura M, Fujii-Kuriyama Y. 1994. Human arylhydrocarbon receptor: functional expression and chromosomal assignment to 7p21. *J Biochem*. 116(4):845–851.

Ema M, Ohe N, Suzuki M, Mimura J, Sogawa K, Ikawa S, Fujii-Kuriyama Y. 1994. Dioxin binding activities of polymorphic forms of mouse and human arylhydrocarbon receptors. *J Biol Chem*. 269(44):27337–27343.

EMBI-EBI. 2020. Ensembl, Release 99: Transcript Summary [Internet]. Hinxton (United Kingdom): EMBL-EBI [cited 2020 Apr 8]. Available from: http://www.ensembl.org/Help/View? id=151. Accessed November 26, 2020.

Flaveny CA, Murray IA, Chiaro CR, Perdew GH. 2009. Ligand selectivity and gene regulation by the human aryl hydrocarbon receptor in transgenic mice. *Mol Pharmacol*. 75(6):1412–1420.

Forgacs AL, Dere E, Angrish MM, Zacharewski TR. 2013. Comparative analysis of temporal and dose-dependent TCDD-elicited gene expression in human, mouse, and rat primary hepatocytes. *Toxicol Sci*. 133(1):54–66.

Freeman DJ, Cattell FCR. 1990. Woodburning as a source of atmospheric polycyclic aromatic hydrocarbons. *Environ Sci Technol*. 24(10):1581–1585.

Fu Q, Li H, Moorjani P, Jay F, Slepchenko SM, Bondarev AA, Johnson PLF, Aximu-Petri A, Prufer K, de Filippo C, et al. 2014. Genome sequence of a 45,000-year-old modern human from western Siberia. *Nature* 514(7523):445–449.

Gee AC, Carlson KE, Martini PGV, Katzenellenbogen BS, Katzenellenbogen JA. 1999. Coactivator peptides have a differential stabilizing effect on the binding of estrogens and antiestrogens with the estrogen receptor. *Mol Endocrinol*. 13(11):1912–1923.

Giani Tagliabue S, Faber SC, Motta S, Denison MS, Bonati L. 2019. Modeling the binding of diverse ligands within the Ah receptor ligand binding domain. *Sci Rep*. 9(1):14.

GraphPad Software. 2020. Prism 8 Curve Fitting Guide: how the AICc computations work [Internet]. San Diego (CA): GraphPad Software [cited 2020 Apr 8]. Available from: https://www.graphpad.com/guides/prism/8/curve-fitting/reg_how_the_aicc_computations_work.htm. Accessed November 26, 2020.

Green RE, Krause J, Briggs AW, Maricic T, Stenzel U, Kircher M, Patterson N, Li H, Zhai W, Fritz MH-Y, et al. 2010. A draft sequence of the neandertal genome. *Science* 328(5979):710–722.

Harper PA, Wong JMY, Lam MSM, Okey AB. 2002. Polymorphisms in the human AH receptor. *Chem Biol Interact*. 141(1–2):161–187.

He B, Kemppainen JA, Wilson EM. 2000. FXXLF and WXXLF sequences mediate the NH2-terminal interaction with the ligand binding domain of the androgen receptor. *J Biol Chem*. 275(30):22986–22994.

He TC, Chan TA, Vogelstein B, Kinzler KW. 1999. PPARdelta is an APC-regulated target of nonsteroidal anti-inflammatory drugs. *Cell* 99(3):335–345.

Heckman KL, Pease LR. 2007. Gene splicing and mutagenesis by PCR-driven overlap extension. *Nat Protoc*. 2(4):924–932.

Helsen C, Claessens F. 2014. Looking at nuclear receptors from a new angle. *Mol Cell Endocrinol*. 382(1):97–106.

Helsen C, Dubois V, Verfaillie A, Young J, Trekels M, Vancraenenbroeck R, De Maeyer M, Claessens F. 2012. Evidence for DNA-binding domain–ligand-binding domain communications in the androgen receptor. *Mol Cell Biol*. 32(15):3033–3043.

Henry AG, Büdel T, Bazin P-L. 2018. Towards an understanding of the costs of fire. *Quat Int*. 493:96–105.

Henry EC, Gasiewicz TA. 2008. Molecular determinants of species-specific agonist and antagonist activity of a substituted flavone towards the aryl hydrocarbon receptor. *Arch Biochem Biophys*. 472(2):77–88.

Hinnebusch AG, Ivanov IP, Sonenberg N. 2016. Translational control by 5′-untranslated regions of eukaryotic mRNAs. *Science* 352(6292):1413–1416.

Hubbard TD, Murray IA, Bisson WH, Lahoti TS, Gowda K, Amin SG, Patterson AD, Perdew GH. 2015. Adaptation of the human aryl hydrocarbon receptor to sense microbiota-derived indoles. *Sci Rep*. 5(1):12689.

Hubbard TD, Murray IA, Bisson WH, Sullivan AP, Sebastian A, Perry GH, Jablonski NG, Perdew GH. 2016. Divergent Ah receptor ligand selectivity during hominin evolution. *Mol Biol Evol*. 33(10):2648–2658.

Köhle C, Bock KW. 2007. Coordinate regulation of Phase I and II xenobiotic metabolisms by the Ah receptor and Nrf2. *Biochem Pharmacol*. 73(12):1853–1862.

Kopec AK, Burgoon LD, Ibrahim-Aibo D, Burg AR, Lee AW, Tashiro C, Potter D, Sharratt B, Harkema JR, Rowlands JC, et al. 2010. Automated dose-response analysis and comparative toxicogenomic evaluation of the hepatic effects elicited by TCDD, TCDF, and PCB126 in C57BL/6 mice. *Toxicol Sci*. 118(1):286–297.

Koyano S, Saito Y, Fukushima-Uesaka H, Ishida S, Ozawa S, Kamatani N, Minami H, Ohtsu A, Hamaguchi T, Shirao K, et al. 2005. Functional analysis of six human aryl hydrocarbon receptor variants in a Japanese population. *Drug Metab Dispos*. 33(8):1254–1260.

Langley E, Kemppainen JA, Wilson EM. 1998. Intermolecular NH2-/carboxyl-terminal interactions in androgen receptor dimerization revealed by mutations that cause androgen insensitivity. *J Biol Chem*. 273(1):92–101.

Liu CC, Xia M, Zhang YJ, Jin P, Zhao L, Zhang J, Li T, Zhou XM, Tu YY, Kong F, et al. 2018. Micro124-mediated AHR expression regulates the inflammatory response of chronic rhinosinusitis (CRS) with nasal polyps. *Biochem Biophys Res Commun*. 500(2):145–151.

Ma Q, Dong L, Whitlock JP. 1995. Transcriptional activation by the mouse Ah receptor: interplay between multiple stimulatory and inhibitory functions. *J Biol Chem*. 270(21):12697–12703.

Mayr C. 2017. Regulation by 3′-untranslated regions. *Annu Rev Genet*. 51(1):171–194.

Meijer FA, Leijten-van de Gevel IA, de Vries RMJM, Brunsveld L. 2019. Allosteric small molecule modulators of nuclear receptors. *Mol Cell Endocrinol*. 485:20–34.

Méjat A, Ramond F, Bassel-Duby R, Khochbin S, Olson EN, Schaeffer L. 2005. Histone deacetylase 9 couples neuronal activity to muscle chromatin acetylation and gene expression. *Nat Neurosci*. 8(3):313–321.

Meyer M, Kircher M, Gansauge MT, Li H, Racimo F, Mallick S, Schraiber JG, Jay F, Prufer K, de Filippo C, et al. 2012. A high-coverage genome sequence from an archaic Denisovan individual. *Science* 338(6104):222–226.

Mishra V, Retherford RD, Smith KR. 2005. Cooking smoke and tobacco smoke as risk factors for stillbirth. *Int J Environ Health Res*. 15(6):397–410.

Moorthy B, Chu C, Carlin DJ. 2015. Polycyclic aromatic hydrocarbons: from metabolism to lung cancer. *Toxicol Sci*. 145(1):5–15.

Moriguchi T, Motohashi H, Hosoya T, Nakajima O, Takahashi S, Ohsako S, Aoki Y, Nishimura N, Tohyama C, Fujii-Kuriyama Y, et al. 2003. Distinct response to dioxin in an arylhydrocarbon receptor (AHR)-humanized mouse. *Proc Natl Acad Sci U S A.* 100(10):5652–5657.

Naeher LP, Brauer M, Lipsett M, Zelikoff JT, Simpson CD, Koenig JQ, Smith KR. 2007. Woodsmoke health effects: a review. *Inhal Toxicol.* 19(1):67–106.

Nakajima M, Iwanari M, Yokoi T. 2003. Effects of histone deacetylation and DNA methylation on the constitutive and TCDD-inducible expressions of the human CYP1 family in MCF-7 and HeLa cells. *Toxicol Lett.* 144(2):247–256.

NCBI. 2017. About RefSeq [Internet]. Bethesda (MD): NCBI [cited 2020 Apr 8]. Available from: https://www.ncbi.nlm.nih.gov/refseq/about/. Accessed November 26, 2020.

Nebert DW, Shi Z, Gálvez-Peralta M, Uno S, Dragin N. 2013. Oral benzo[a]pyrene: understanding pharmacokinetics, detoxication, and consequences—*Cyp1* knockout mouse lines as a paradigm. *Mol Pharmacol.* 84(3):304–313.

Nukaya M, Bradfield CA. 2009. Conserved genomic structure of the Cyp1a1 and Cyp1a2 loci and their dioxin responsive elements cluster. *Biochem Pharmacol.* 77(4):654–659.

Okey AB, Franc MA, Moffat ID, Tijet N, Boutros PC, Korkalainen M, Tuomisto J, Pohjanvirta R. 2005. Toxicological implications of polymorphisms in receptors for xenobiotic chemicals: the case of the aryl hydrocarbon receptor. *Toxicol Appl Pharmacol.* 207(2):43–51.

Okey AB, Vella LM, Harper PA. 1989. Detection and characterization of a low affinity form of cytosolic Ah receptor in livers of mice nonresponsive to induction of cytochrome P1-450 by 3-methylcholanthrene. *Mol Pharmacol.* 35(6):823–830.

Pandini A, Denison MS, Song Y, Soshilov AA, Bonati L. 2007. Structural and functional characterization of the aryl hydrocarbon receptor ligand binding domain by homology modeling and mutational analysis. *Biochemistry* 46(3):696–708.

Pohjanvirta R, Wong JM, Li W, Harper PA, Tuomisto J, Okey AB. 1998. Point mutation in intron sequence causes altered carboxyl-terminal structure in the aryl hydrocarbon receptor of the most 2,3,7,8-tetrachlorodibenzo-p-dioxin-resistant rat strain. *Mol Pharmacol.* 54(1):86–93.

Poland A, Glover E. 1990. Characterization and strain distribution pattern of the murine Ah receptor specified by the *Ahd* and *Ahb-3* alleles. *Mol Pharmacol.* 38(3):306–312.

Poland A, Palen D, Glover E. 1994. Analysis of the four alleles of the murine aryl hydrocarbon receptor. *Mol Pharmacol.* 46(5):915–921.

Prager M, Buttner J, Grunert P, Ellinghaus D, Buning C. 2016. A promoter variant within the aryl hydrocarbon receptor gene is associated with an epithelial barrier defect in smokers with Crohn's disease. *Inflamm Bowel Dis.* 22(10):2356–2368.

Procopio M, Lahm A, Tramontano A, Bonati L, Pitea D. 2002. A model for recognition of polychlorinated dibenzo-p-dioxins by the aryl hydrocarbon receptor. *Eur J Biochem.* 269(1):13–18.

Prüfer K, de Filippo C, Grote S, Mafessoni F, Korlevic P, Hajdinjak M, Vernot B, Skov L, Hsieh P, Peyregne S, et al. 2017. A high-coverage Neandertal genome from Vindija Cave in Croatia. *Science* 358(6363):655–658.

Prüfer K, Racimo F, Patterson N, Jay F, Sankararaman S, Sawyer S, Heinze A, Renaud G, Sudmant PH, de Filippo C, et al. 2014. The complete genome sequence of a Neanderthal from the Altai Mountains. *Nature* 505(7481):43–49.

Roberts EA, Johnson KC, Harper PA, Okey AB. 1990. Characterization of the Ah receptor mediating aryl hydrocarbon hydroxylase induction in the human liver cell line Hep G2. *Arch Biochem Biophys.* 276(2):442–450.

Roebroeks W, Villa P. 2011. On the earliest evidence for habitual use of fire in Europe. *Proc Natl Acad Sci U S A.* 108(13):5209–5214.

Sambrook J, Russell DW. 2001. Molecular cloning: a laboratory manual. Cold Spring Harbor (NY): Cold Spring Harbor Laboratory Press.

Sandgathe DM, Dibble HL, Goldberg P, McPherron SP, Turq A, Niven L, Hodgkins J. 2011. Timing of the appearance of habitual fire use. *Proc Natl Acad Sci U S A.* 108(29):E298–E298.

Senapati D, Kumari S, Heemers HV. 2020. Androgen receptor co-regulation in prostate cancer. *Asian J Urol.* 7(3):219–232.

Seok S-H, Lee W, Jiang L, Molugu K, Zheng A, Li Y, Park S, Bradfield CA, Xing Y. 2017. Structural hierarchy controlling dimerization and target DNA recognition in the AHR transcriptional complex. *Proc Natl Acad Sci U S A.* 114(21):5431–5436.

Shao D, Rangwala SM, Bailey ST, Krakow SL, Reginato MJ, Lazar MA. 1998. Interdomain communication regulating ligand binding by PPAR-γ. *Nature* 396(6709):377–380.

Shimelmitz R, Kuhn SL, Jelinek AJ, Ronen A, Clark AE, Weinstein-Evron M. 2014. 'Fire at will': the emergence of habitual fire use 350,000 years ago. *J Hum Evol.* 77:196–203.

Silkworth JB, Koganti A, Illouz K, Possolo A, Zhao M, Hamilton SB. 2005. Comparison of TCDD and PCB CYP1A induction sensitivities in fresh hepatocytes from human donors, sprague-dawley rats, and rhesus monkeys and HepG2 cells. *Toxicol Sci.* 87(2):508–519.

Singh SS, Hord NG, Perdew GH. 1996. Characterization of the activated form of the aryl hydrocarbon receptor in the nucleus of HeLa cells in the absence of exogenous ligand. *Arch Biochem Biophys.* 329(1):47–55.

Sorensen AC. 2017. On the relationship between climate and Neandertal fire use during the Last Glacial in south-west France. *Quat Int.* 436(Part A):114–128.

Sorensen AC, Claud E, Soressi M. 2018. Neandertal fire-making technology inferred from microwear analysis. *Sci Rep.* 8(1):10065.

Tsuchiya Y, Nakajima M, Itoh S, Iwanari M, Yokoi T. 2003. Expression of aryl hydrocarbon receptor repressor in normal human tissues and inducibility by polycyclic aromatic hydrocarbons in human tumor-derived cell lines. *Toxicol Sci.* 72(2):253–259.

Van den Berg M, Birnbaum LS, Denison M, De Vito M, Farland W, Feeley M, Fiedler H, Hakansson H, Hanberg A, Haws L, et al. 2006. The 2005 World Health Organization re-evaluation of human and mammalian toxic equivalency factors for dioxins and dioxin-like compounds. *Toxicol Sci.* 93(2):223–241.

Vorrink SU, Hudachek DR, Domann FE. 2014. Epigenetic determinants of CYP1A1 induction by the aryl hydrocarbon receptor agonist 3,3',4,4',5-pentachlorobiphenyl (PCB 126). *Int J Mol Sci.* 15(8):13916–13931.

Whitelaw ML, Gustafsson JA, Poellinger L. 1994. Identification of transactivation and repression functions of the dioxin receptor and its basic helix-loop-helix/PAS partner factor ARNT: inducible versus constitutive modes of regulation. *Mol Cell Biol.* 14(12):8343–8355.

Whitlock MC. 2000. Fixation of new alleles and the extinction of small populations: drift load, beneficial alleles, and sexual selection. *Evolution* 54(6):1855–1861.

Wiessner P. 2014. Embers of society: firelight talk among the Ju/'hoansi Bushmen. *Proc Natl Acad Sci U S A.* 111(39):14027–14035.

Wincent E, Bengtsson J, Bardbori AM, Alsberg T, Luecke S, Rannug U, Rannug A. 2012. Inhibition of cytochrome P4501-dependent clearance of the endogenous agonist FICZ as a mechanism for activation of the aryl hydrocarbon receptor. *Proc Natl Acad Sci U S A.* 109(12):4479–4484.

Wrangham R. 2009. Catching fire: how cooking made us human. New York: Basic Books.

Wrangham R, Carmody R. 2010. Human adaptation to the control of fire. *Evol Anthropol.* 19(5):187–199.

Zeiger M, Haag R, Höckel J, Schrenk D, Schmitz HJ. 2001. Inducing effects of dioxin-like polychlorinated biphenyls on CYP1A in the human hepatoblastoma cell line HepG2, the rat hepatoma cell line H4IIE, and rat primary hepatocytes: comparison of relative potencies. *Toxicol Sci.* 63(1):65–73.

Zhang S, Rowlands C, Safe S. 2008. Ligand-dependent interactions of the Ah receptor with coactivators in a mammalian two-hybrid assay. *Toxicol Appl Pharmacol.* 227(2):196–206.

Zhou ZX, Lane MV, Kemppainen JA, French FS, Wilson EM. 1995. Specificity of ligand-dependent androgen receptor stabilization: receptor domain interactions influence ligand dissociation and receptor stability. *Mol Endocrinol.* 9(2):208–218.